VOL. 11, NO. 4, FEBRUARY 2016 ISSN 1819-6608
ARPN Journal of Engineering and Applied Sciences


www.arpnjournals.com

ACOUSTIC SIGNAL STRENGTH FOR DAMAGE EVALUATION OF REINFORCED CONCRETE BEAM

Noorsuhada Md Nor and Soffian Noor Mat Saliah
Faculty of Civil Engineering Universiti Teknologi Mara Pulau Pinang, Permatang Pauh, Pulau Pinang, Malaysia
E-Mail: idanur211@gmail.com

ABSTRACT

Reinforced concrete (RC) structure is a common material used in construction and exposed to excessive load over time. The load would generate cracks in the RC structure and need to be evaluated. This paper presents an acoustic emission (AE) monitoring for damage evaluation of RC beam subjected to increasing fatigue loading. The fatigue loading is subjected on the RC beam based on six loading phases. A total of twelve samples were tested using three-point loading and evaluated using AE signal strength parameter. The AE signal strength is evaluated at flexural region and shear region. Visual crack pattern appeared on the beam surface is also observed. It is found that the AE signal strength to demonstrate the occurrence of crack initiation and propagation in the tested specimen is well matched with the visual observation. Hence, the AE analysis based on signal strength provides valuable information on the occurrence of damage in the RC beam.

Keywords: acoustic emission, signal strength, damage assessment.

INTRODUCTION

Acoustic emission signal strength is defined as "the measured area of the rectified AE signal with units proportional to volt-seconds" (ASTM, 2006) and one type of the AE energies. Ziehl (2000) stated the signal strength normally includes the absolute area of the positive and negative envelopes. It relates to the relative energy released by the specimen and rely on function of the amplitude and duration of the signal (Xu, 2008). It can be defined using equation (1), where f+ is the positive signal envelope function, f- is the negative signal envelope function, t1 is time at first threshold crossing and t2 is the time at last threshold crossing.

$$S_0 = \frac{1}{2}\int_{t_1}^{t_2} f_+(t)\,dt - \frac{1}{2}\int_{t_1}^{t_2} f_-(t)\,dt \quad (1)$$

The application of AE signal strength for damage evaluation of RC structure has been earlier reviewed by Md Nor *et al.* (2011). They found that the condition of RC beam can be predicted and forthcoming of cracks in the structure can be inspected. According to Xu (2008), the cumulative signal strength versus time can be used for damage evaluation and determination of integrity of prestressed concrete structure. Chotickai (2001) enhanced that signal strength can also be used for damage evaluation of prestressed bridge girder. Ziehl (2000) affirmed that the AE onset on fibre reinforced vessel can be determined using signal strength. Seo and Kim (2008) found that the cumulative AE energy able to determine the fatigue damage and healing stage in asphalt concrete. Meanwhile, Shigeishi *et al.* (2001) stated that the characteristic of masonry bridge and concrete bridge can be determined using AE energy.

The application of signal strength in assessing the structure condition is more significant if other external parameters such as load, deflection and strain that induce the AE can be analysed together. For instance, Chotickai (2001) has analysed signal strength versus load for determination of damage occurrence in the prestressed bridge girder. Cumulative signal strength, historic index versus time has been used to determine the significant damage in RC beam subjected to cyclic load by Nair (2006). The same analysis also has been used by Gostautas *et al.* (2005) to determine the structural performance of the glass fibre reinforced composites bridge decks during in-service field inspection. They stated that the analysis can be used to identify the possible damage mechanisms and the onset of failure in the bridge decks. The signal strength has been used by Shahidan *et al.* (2012) in intensity analysis for determination of damage intensity of RC beam when subjected to stepwise loading.

The cumulative signal strength has been imposed on historic index and severity as a function of time to monitor external bonded carbon fibre reinforced polymer used for repair reinforced concrete slab by Degala *et al.* (2009). Several types of damages as well as initiation, progression and localization were determined. The onset of damage can also be predicted. AE signal strength with respect to normalized cycles has been used by Md Nor *et al.* (2014) in determination of fatigue damage initiation, steady stage and failure stage of RC beam specimen subjected to two constant fatigue loads until failure. The first fatigue load was based on $0.7P_{ult}$ and the second was $0.8P_{ult}$. They found that AE signal strength subjected to $0.8P_{ult}$ is higher than that of $0.7P_{ult}$. Currently, energy, event number versus normalized elapsed time has been analysed to determine the structural integrity and micro damage of carbon fibre reinforced polymer (CFRP) by Choi and Yun (2015).

From the reviews indicate that the analysis based on AE signal strength is still relevant to date and can be used for damage evaluation of RC structure. Hence, the main objective of this paper is to gain better understanding and enhance the experiment database of

crack behaviour of RC beam specimen subjected to increasing fatigue loading in conjunction with signal strength of AE.

EXPERIMENTAL PROGRAMME AND AE ANALYSIS

A total of twelve reinforced concrete (RC) beams were fabricated in 150 mm x 150 mm x 750 mm sections with a specified design compressive strength of 40 N/mm^2 for all specimens. The same preparation of RC beam specimens, testing procedures, load protocols, visual inspection of crack observation and AE monitoring as presented by Md Nor *et al.* (2013) were also presented in this paper. However, the different was the AE analysis correlates to the visual inspection of the crack pattern.

The fatigue test was performed using servo-hydraulic testing machine. The test was based on a sine wave load cycle with the frequency of 1 Hz and six phases of loads were applied. Each phase, the beam was loaded 5000 fatigue cycles. The six load phases of the fatigue tests are depicted in Table-1. The maximum fatigue loadings were based on the load at first crack, P_{cr} and ultimate static load, P_{ult}. The same load protocol also has been implemented by Md Nor (2014) and Md Nor *et al.* (2013).

During fatigue test and AE monitoring, the crack patterns were observed. The crack occurrence was visualized and marked when all the machine and AE system paused. The cracks appeared on the beam specimen marked with numbers 1 to 6 indicates the crack pattern corresponding to Phase 1 to Phase 6 of loading.

In this paper, the AE analysis was based on the application of AE signal strength to assess the fatigue damage. The analysis was carried out for each phase of loadings. The analysis was based on the analysis of signal strength versus load cycles and cumulative signal strength versus load cycles. The analysis was carried out based on the AE signal strength collected at Channel 3 (CH3). This is because CH3 has collected high AE activity since it was the closest sensor to the critical crack area. It is also the channel that captured more energy than the other sensors. The signal obtained from the closest sensor to AE source was the one considered to reduce the effect of attenuations (2012). Figure–1 shows the arrangement of the AE sensors on the RC beam specimen.

Table-1. Summary of three (3) phases for each stage of maximum fatigue load applied to the beam specimens size 150 mm x 150 mm x 750 mm.

Stage 1: Applied load based on P_{cr}			Stage 2: Applied load based on P_{ult}		
Load Phases	Load Ratio	P_{max} (kN)	Load Phases	Load Ratio	P_{max} (kN)
Phase 1	0.5	12	Phase 4	0.2	32
Phase 2	0.8	19	Phase 5	0.5	63
Phase 3	1.0	24	Phase 6	0.6	79

RESULTS AND DISCUSSION

Crack Observation

Figure-2 shows the crack observation of the RC beam specimen under six phases of fatigue loadings. The cracks progressively increased as the load increased. When maximum fatigue loading of 12 kN (Phase 1) was applied on the beam specimen, the first crack was developed at the centre of the beam and designated as 1 as shown in Figure-2a. The crack at mid-span of the beam was propagated almost vertically beyond neutral axis. According to McCormac and Nelson (2006), if the crack occurs beyond neutral axis, it means the reinforcing bars have yielded. This indicated that low fatigue load amplitude based on P_{cr} could develop crack in the RC beam.

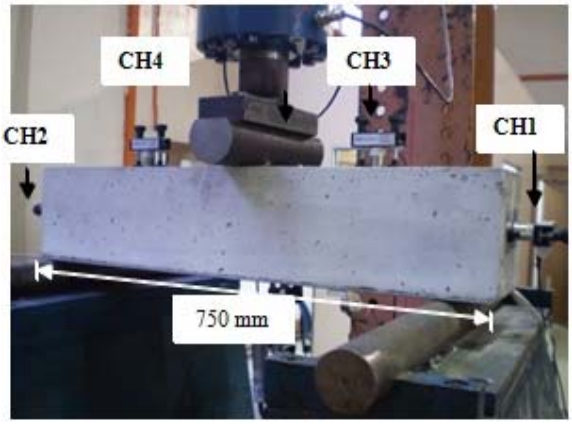

Figure-1. RC beam setup and location of sensors.

The second crack was occurred as the loading phase 2 (19 kN) applied and designated as 2. The crack number 2 was propagated from tip of the preceding crack and a new crack was developed vertically at where shear cracks normally occurred. It can be seen in Figure-2b where the crack occurred at 0.236 m from CH1.

When the RC beam specimen subjected to 24 kN designated as Phase 3 loading, more new cracks were developed as shown in Figure-2c. The crack that occurred in the shear region started to propagate diagonally from the previous crack that occurred when subjected to Phase 2 loading. The shear crack started to propagate diagonally when the beam specimen subjected to 32 kN under Phase 4 loading. At this phase, no new crack occurred at the bottom of the beam specimen as shown in Figure-2d. Most of the cracks were propagated from the tip of the previous cracks under precious loadings. However, in the flexural region, no new crack was propagated from the tip of the crack Number 3 as denoted on the beam specimen shown in Figure-2d.

More diagonal cracks known as shear cracks were developed and propagated from supports to the point load at the top of the beam specimen when 63 kN was applied. It can be seen in Figure. 2e by crack marked as Number 5. Pimanmas (2007) stated that when the flexural

crack becomes inactive, a large shear crack is formed. The length of crack is propagated by a small increase of crack that was visually inspected when the beam was subjected to 79 kN as shown in Figure-2f.

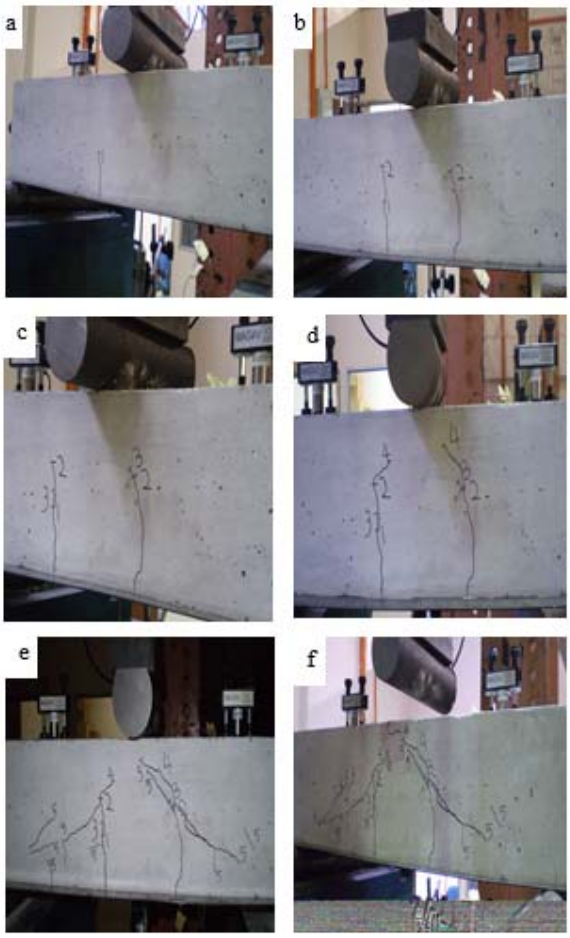

Figure-2. Crack pattern of RC beam subjected to increasing fatigue load range a) Phase 1 ($0.5P_{cr}$); b) Phase 2 ($0.8P_{cr}$); c) Phase 3 ($1.0P_{cr}$); d) Phase 4 ($0.2P_{ult}$); e) Phase 5 ($0.5P_{ult}$); and f) Phase 6 ($0.6P_{ult}$).

Signal Strength of Acoustic Emission

Figure-3 shows a trend of AE characteristic by signal strength corresponding to different maximum fatigue load with respect to load cycles. In the Phase 1 loading of $0.5P_{cr}$, the signal strength of 9660 nVs was observed when the first flexural crack appeared on the RC beam surface. The highest signal strength was recorded from the beam under Phase 2 loading or when the beam was subjected to $0.8P_{cr}$. It obviously matched the occurrence of the vertical direction of flexural crack. When diagonal shear crack occurred, the signal strength versus X-location produced low value since the signal strength moved sideways. The signal strength of 9660 nVs was recorded when the beam was subjected to 82 load cycles and it indicates the occurrence of the first flexural crack.

Corresponding to the relationship between signal strength and load cycles as shown in Figure-3, it is found that significant spikes of AE with high signal strength of 52500 nVs at load cycles of 9358 can be related to the fatigue damage in the RC beam specimens. As stated by Degala (2008), the significant spikes of signal strength can be used to identify the possible damage mechanism and the occurrence of failure. Corresponding to the present result, it is where the extension of flexural crack occurred at the mid-span from the previous crack and the occurrence of new crack in the shear region. A sudden increase of signal strength during application of Phase 4 loading or beam subjected to $0.2P_{ult}$, the spike of AE signal strength at 16857 cycles with 29300 nVs indicates the occurrence of shear cracks in the beams.

The highest value of signal strength has occurred at the 9358 load cycles. If the crack pattern is referred to as discussed in the preceding paragraph (see Figure-2b), the flexural crack in the mid-span of the beam was propagated beyond the mid-depth of the beam. It indicates that the highest value of signal strength depict the development of macrocracks in the concrete.

As the load cycle increases to 10000 cycles, higher signal strength were recorded. More cracks were also generated and propagated in the RC beam specimen. The first shear crack occurred when the load reaches 10201 cycles. After that load cycles, the shear crack continuously progressing.

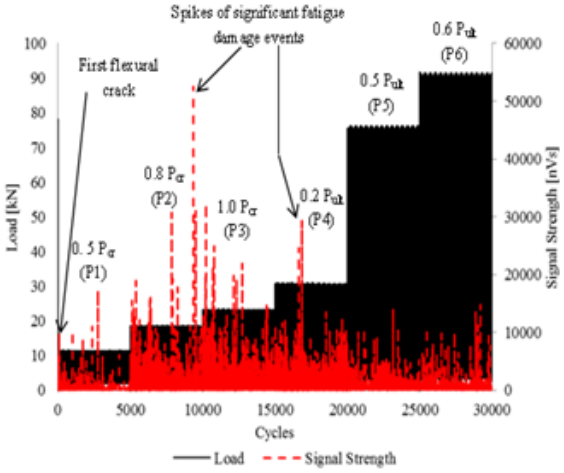

Figure-3. Load, signal strength versus load cycles for beam size of 150 mm x 150 mm x 750 mm.

Figure-4 shows the typical example of how the AE signal strength accumulates during the six (6) groups of maximum fatigue loads applied on the beam specimen with the same load cycles and the fatigue frequency. This accumulation is particularly vital to describe the damage progression in the beam specimen. The rate of the emission is dependent upon the rate of applied load (2001). Figure-4 shows that a significant increase of cumulative signal strength (CSS) started when $0.8P_{cr}$ was

applied on the beam specimen. It can be related to the fatigue failure threshold. Bourchak *et al.* (2007) stated that sudden spike of cumulative AE energy is considered as the fatigue failure thresholds which is associated with the significant change of damage accumulation with respect to the AE energy history.

The findings reported by Bourchak *et al.* (2007) are similar to this graph of cumulative signal strength with respect to load cycles, where a sudden increase is noticed between Phase 1 and Phase 2 loadings. Then, the graph is almost linear when the beam specimen was subjected to $0.2P_{ult}$ (Phase 4). Another significant change can be observed when the beam was imposed to $0.5P_{ult}$ loading. It might be due to progressive damage by shear crack in the beam specimen. Then, the cumulative signal strength progressively increases when $0.6P_{ult}$ was applied.

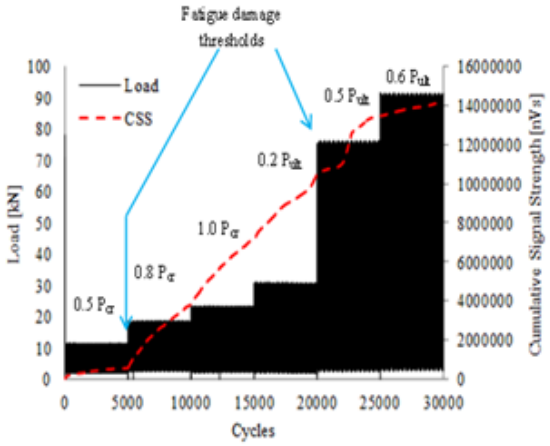

Figure-4. Load and cumulative signal strength (css) versus load cycles for beam size of 150 mm x 150 mm x 750 mm.

Based on the trend of AE signal strength for each load phase explained in the preceding sections, a summary can be made to identify the damage level of the beam under fatigue loading. Since the plots of signal strength is scattered with high intensity, a certain highest value of signal strength corresponding to the distance can be made. The summary is tabulated in Table-2. Overall, the signal strength that is associated with flexural crack increases as the load increases for the first two (2) phases. When the load increases, the highest value of signal strength captured along 0.31 m to 0.44 m becomes constant. The generation of new crack along this distance produced low signal strength.

For shear crack occurred in distance between 0.1 m to 0.3 m, the highest signal strength was recorded from 9600 nVs under Phase 1 loading and the value increased to 24900 nVs when the maximum fatigue increased to Phase 3 loading and no increase in signal strength was recorded after that phases. It indicates that although shear crack was progressively occurred, in which is diagonally propagated from the support to the point of load, it produced very low signal strength because the signal strength have moved sideways (2008). Similar situation was observed at the other side of shear crack region which is in between 0.45 m to 0.65 m distance from the most left of the edge where the signal strength increased as the load increases. The highest value of signal strength becomes constant as Phase 4 loading and onwards was applied. Therefore, it can be deduced that the signal strength is useful in the determination of location of crack and the determination of progression of shear crack.

Table-2. Summary of highest value of signal strength at flexural region and shear region for beam specimen 150 mm x 150 mm x 750 mm.

Load	Phase	Highest Value of Signal Strength (nVs) and location (m)		
		Flexural Region (0.31 m – 0.44 m)	Shear Region (0.1 m – 0.3 m)	Shear Region (0.45 m - 0.65 m)
$0.5P_{cr}$	1	17300 (0.37)	9660 (0.18)	2680 (0.46)
$0.8P_{cr}$	2	52500 (0.37)	19300 (0.18)	6490 (0.45)
$1.0P_{cr}$	3	52500 (0.37)	24900 (0.16)	8920 (0.58)
$0.2P_{ult}$	4	52500 (0.37)	24900 (0.16)	16200 (0.57)
$0.5P_{ult}$	5	52500 (0.37)	24900 (0.16)	16200 (0.57)
$0.6P_{ult}$	6	52500 (0.37)	24900 (0.16)	16200 (0.57)

CONCLUSIONS

Based on testing results on the RC beam specimens, the following conclusions can be drawn from the investigation of the fatigue crack progression corresponding to the AE signal strength when subjected to increasing fatigue loading:

(i) It is deduced that the crack increases as the load applied on the beam specimen increases.

(ii) It is found that the first flexural crack occurred beyond the mid-depth of the RC beam specimens when the load $0.5P_{cr}$ was applied. The concentration of the crack was found at the area of the mid-span of the beam.

(iii) The cumulative signal strength versus time was found dependent upon the load application and two cracks can be identified.

REFERENCES

[1] ASTM, E. 1316. (2006). Standard terminology for nondestructive examinations. ASTM International.

[2] Bourchak, M., Farrow, I. R., Bond, I. P., Rowland, C. W., & Menan, F. (2007). Acoustic emission energy as

a fatigue damage parameter for CFRP composites. International Journal of Fatigue, 29, 457–470.

[3] Choi, W.C. and Yun, H.D. (2015). Acoustic emission activity of CFRP-strengthened reinforced concrete beams after freeze–thaw cycling, cold Regions Science and Technology, 110, 47–58.

[4] Chotickai, P. (2001). Acoustic Emission Monitoring of Prestressed Bridge Girders with Premature Concrete Deterioration. Master of Science in Engineering, The University of Texas.

[5] Degala, S. (2008). Acoustic emission monitoring of reinforced concrete systems retrofitted with CFRP. Master of Science, University of Pittsburgh.

[6] Degala, S. Rizzo, P., Ramanathan, K., Harries, K.A. (2009) Acoustic emission monitoring of CFRP reinforced concrete slabs. Construction and Building Materials, 23, 2016-2026.

[7] Gostautas, R. S., Ramirez, G., Peterman, R. J., & Meggers, D. (2005). Acoustic emission monitoring and analysis of glass fiber-reinforced composites bridge decks. Journal of Bridge Engineering, 10(6), 713–721.

[8] McCormac, J. C., & Nelson, J. K. (2006). Design of reinforced concrete ACI 318-05 Code edition.

[9] Md Nor, N. (2014). Fatigue damage assessment of reinforced concrete beam using acoustic emission technique, PhD Thesis, Universiti Teknologi MARA, Malaysia.

[10] Md Nor, N. Ibrahim, A., Muhamad Bunnori, N., Mohd Saman, H., Mat Saliah, S.N., Shahidan, S. (2014) Diagnostic of fatigue damage severity on reinforced concrete beam using acoustic emission technique, Engineering Failure Analysis 41, 1–9

[11] Md Nor, N., Ibrahim, A., Muhamad Bunnori, N., Mohd Saman, H., Mat Saliah, S.N., Shahidan, S. (2013) Active Fatigue Crack Detection and Classification of Reinforced Concrete Beams using Acoustic Emission. Proceedings of the International Civil and Infrastructure Engineering Conference, 21st - 25th September, 2013 in Pullman Kuching, Sarawak, Malaysia.

[12] Md Nor, N., Muhamad Bunnori, N., Ibrahim, A., Shahidan, S. and Mat Saliah, S.N. (2011). Relationship between acoustic emission signal strength and damage evaluation of reinforced concrete structure: Case studies, 2011 IEEE Symposium on Industrial Electronics and Applications (ISIEA2011), September 25-28, 2011, Langkawi, Malaysia.

[13] Momon, S., Godin, N., Reynaud, P., R'mili, M., & Fantozzi, G. (2012). Unsupervised and supervised classification of AE data collected during fatigue test on CMC at high temperature. Composites Part A, 43, 254–260.

[14] Muhamad Bunnori, N. (2008). Acoustic emission techniques for the damage assessment of reinforced concrete structures. Phd Thesis, Cardiff University.

[15] Nair, A. (2006). Acoustic emission monitoring and quantitative evaluation of damage in reinforced concrete members and bridges. Master of Science in Civil Engineering, Kerala University.

[16] Pimanmas, A., Behaviour and failure mode of reinforced concrete members damaged by pre-cracking. Songklanakarin J. Sci. Technol., 2007. 29(4): p. 1039-1048

[17] Seo, Y., & Kim, R. Y. (2008). Using acoustic emission to monitor fatigue damage and healing in asphalt concrete. KSCE Journal of Civil Engineering, 237–243.

[18] Shahidan, S., Muhamad Bunnori, N., Md Nor, N. & Mohd Basri, S.R. (2012). Health index evaluation on acoustic emission signal for concrete structure by intensity analysis method. Advanced Materials Research, 403-408 (2012), 3729-3733.

[19] Shigeishi, M., Colombo, S., Broughton, K. J., Rutledge, H., Batchelor, A. J., & Forde, M. C. (2001). Acoustic emission to assess and monitor the integrity of bridges. Construction and Building Materials, 15, 35–49.

[20] Xu, J. (2008). Nondestructive evaluation of prestressed concrete structures by means of acoustic emissions monitoring. PhD Thesis. Auburn University.

[21] Ziehl, P. H. (2000). Development of a damage based design criterion for fiber reinforced vessels. PhD Thesis. The University of Texas.